CI/FSK: Bandwidth-Efficient Multicarrier FSK for High Performance, High Throughput, and Enhanced Applicability

Balasubramaniam Natarajan, *Member, IEEE*, Carl R. Nassar, *Senior Member, IEEE*, and Steve Shattil

***Abstract*—In traditional binary frequency-shift keying (BFSK), two distinct carrier frequencies are used to represent binary data. In this letter, we propose transmitting multiple orthogonal, in-phase subcarriers around two distinct carrier frequencies to represent binary information. The envelope of the resulting FSK signal is a carrier interferometry pattern, and hence, the name carrier interferometry (CI/) FSK. We demonstrate that this technique is spectrally efficient when compared to traditional BFSK. Performance and data-rate benefits are also demonstrated with the use of a novel coherent reception technique. Moreover, while it is difficult to employ traditional BFSK in multipath channels, we show how the new CI/FSK scheme exploits frequency-diversity benefits when used in such channels.**

***Index Terms*—Carrier interferometry (CI), multicarrier (MC) modulation, frequency-shift keying (FSK).**

I. Introduction

FREQUENCY-SHIFT keying (FSK) is a modulation technique of great practical importance. It is commonly used whenever the hardware simplicity of the receiver is of utmost importance [1]. Recently, FSK has gained popularity with its adoption in the Bluetooth standard [2]–[4]. The selection of FSK for personal area networks (such as Bluetooth) was motivated by a number of considerations. Noncoherent FSK receivers can be designed with ease and can be implemented in a cost-effective manner. Since most FSK modulation techniques result in a constant envelope, information is carried by the zero crossings of the signal alone. Hence, FSK is robust in systems that have nonlinearities due to, e.g., radio frequency (RF) amplifier effects [5].

However, FSK also has significant disadvantages. Since the binary FSK (BFSK) constellation is orthogonal rather than antipodal, it suffers from a 3-dB penalty in signal-to-noise ratio (SNR) for a given bit-error rate (BER) [when compared with coherent binary phase-shift keying (BPSK)]. Additionally, the spectral efficiency of FSK is often lower than passband pulse-amplitude modulation (PAM) and phase-shift keying (PSK). Next, since the basic FSK signal is not a linear function of the data, existing linear-equalization techniques cannot be used. Hence, compensation for channel distortion like selective fading is more difficult in FSK. As a result, multipath channels introduce an error floor (even in the absence of noise) [6]. This major drawback hinders the widespread use of FSK in wireless systems [1].

There has been considerable interest in designing FSK detectors for multipath channels (see [7]–[12]). In [7], an asymmetric raised-cosine pulse shape is applied, as is a limiter discriminator receiver, improving the performance of FSK in multipath channels with small delay spreads. However, when the delay spread increases above the symbol duration, a significant error floor appears. Additionally, the system in [7] introduces a nominal degradation in spectral efficiency relative to Gaussian FSK (GFSK). In [8], performance gains in Rayleigh fading channels with small interpath delays are achieved via a quadratic decorrellation receiver. In [9], a generalization of frequency modulation (FM) noise-click theory is used to design an FSK receiver for detection after multipath spreading. In both [8] and [9], there is significant degradation in performance when the delay spread approaches symbol duration. A novel noncoherent equalizer for FSK is introduced in [10]. Here, intersymbol interference (ISI) is combated using an approach similar to the phase-independent decorrellator multiuser detection employed in multiple-access systems (where interference from other users is *tuned out*). However, just as in multiuser detection, complexity is a limiting factor in this approach. Recently, in [11] and [12], the idea of exploiting path diversity in FSK systems is explored, and it is shown to yield nominal performance gains. The impact of interpath interference, along with hardware limitations (restricting the number of RAKE fingers that can be implemented), reduces this system's ability to benefit from the available diversity.

In this letter, we propose an enhancement to BFSK that: 1) provides improved spectral efficiency; 2) supports enhanced BER performance; and 3) ensures the successful transmission of FSK over frequency-selective channels, by supporting frequency diversity benefits.

Specifically, in traditional BFSK, carrier frequency $f_c + f_d$ represents binary "1," and carrier frequency $f_c - f_d$ indicates binary "0." In the new system, we use N orthogonal in-phase subcarriers around $f_c + f_d$ to represent one, and a second set of N subcarriers centered about $f_c - f_d$ to represent zero. The total transmitted signal has an average frequency equal to either $f_c + f_d$ or $f_c - f_d$, while the envelope corresponds to a carrier interferometry (CI) pattern. Hence, this novel FSK system is referred to as carrier interferometry/FSK (CI/FSK), and can be understood as a synergistic combination of orthogonal frequency-division multiplexing (OFDM) and FSK.

We first demonstrate that CI/FSK has a spectral efficiency comparable to that of FM with a $\mathrm{sinc}(\cdot)$ modulating waveform,

Paper approved by C. Tellambura, the Editor for Modulation and Signal Design of the IEEE Communications Society. Manuscript received January 28, 2002; revised August 8, 2003. This paper was presented in part at the IEEE International Conference on Communications, New York, NY, May 2002.

B. Natarajan is with the Department of Electrical and Computer Engineering, Kansas State University, Manhattan, KS 66506-5204 USA (e-mail: bala@eece.ksu.edu).

C. R. Nassar is with the Department of Electrical and Computer Engineering, Colorado State University, Ft. Collins, CO 80523-1373 USA (e-mail: carln@engr.colostate.edu).

S. Shattil is with Idris Communications, Boulder, CO 80301 USA (e-mail: steve@idriscomm.com).

Digital Object Identifier 10.1109/TCOMM.2004.823570

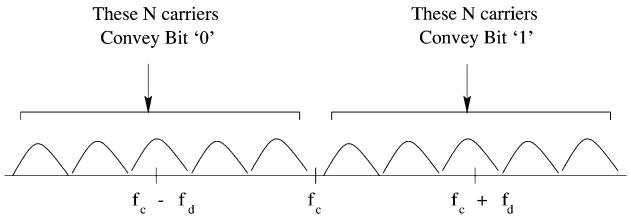

Fig. 1. CI/FSK signal sent for bit zero (on the left) and bit one (on the right). Each signal is the linear combination of N carriers.

and hence, can support higher data rates in a given bandwidth relative to BFSK. Specifically, given a total system bandwidth, $\mathrm{BW}_{\mathrm{total}}$, a CI/FSK system can support data rates that are 100% and 35% higher than a traditional BFSK and GFSK $(\mathrm{BT} = 0.3)$ system, respectively. We then analyze the crest factor [13] of the transmitted signal, and show how the nonconstant envelope is eliminated when a bit stream is transmitted using CI/FSK modulation. The crest factor of the CI/FSK signal, when considering transmission of a bit stream, is shown to be equal to that of a single sine wave.

Next, we demonstrate how the throughput of CI/FSK can be doubled, without bandwidth expansion and with small performance degradation, by extending the concept of pseudo-orthogonality (used with success in code-division multiple-access (CDMA) systems). Specifically, by positioning the CI/FSK modulated symbols pseudo-orthogonally at the transmitter, the number of transmitted symbols is doubled. This intentional introduction of ISI at the transmitter is effectively countered by employing the novel coherent CI/FSK receiver introduced in this letter.

It is important to note that the gains achieved using the CI/FSK approach come at a cost of a moderate increase in complexity, relative to traditional BFSK systems. However, CI/FSK's multicarrier (MC) OFDM-like transmission/reception can exploit the low complexity inverse fast Fourier transform/fast Fourier transform (IFFT/FFT)-based transceiver implementation (as currently available for OFDM).

II. CI/FSK Signaling

A. Frequency and Time Representation

In CI/FSK, two nonoverlapping frequency bands with center frequencies $f_c + f_d$ and $f_c - f_d$ convey binary information, similar to BFSK. However, unlike BFSK, the CI/FSK transmitter sends N orthogonal in-phase subcarriers centered around $f_c + f_d$ (for bit one) or $f_c - f_d$ (for bit zero). This is shown conceptually in Fig. 1. To maintain orthogonality between subcarriers, we select $\Delta f = (1/NT_b)$, where T_b is the bit duration. This frequency spacing will create overlap between subcarriers (much like OFDM [14], but not shown in Fig. 1), which, in turn, enhances bandwidth efficiency (as discussed in Section II-D).

With N subcarriers used to represent bit zero and bit one, and subcarrier spacing set to $\Delta f = (1/NT_b)$, an important design parameter is the selection of N. The value of N is chosen to: 1) ensure a flat fade over each subcarrier (just as in OFDM systems [15]); and 2) maintain a reasonable time duration over which bit energy is spread. Refering to criteria 1), in which we require a flat fade over each subcarrier, we note that the

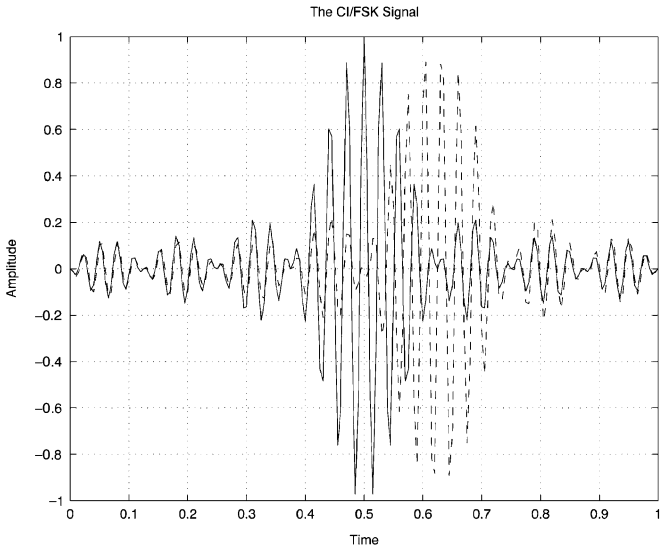

Fig. 2. Solid line is one CI/FSK signal. Dashed line is a time-shifted CI/FSK signal (shifted by a bit duration T_b).

frequency width of each subcarrier is $\Delta f = (\mathrm{BW}_{\mathrm{total}}/2N)$, e.g., $\Delta f = (1.4/2N)$ MHz $= (700/N)$ kHz. Additionally, considering a typical urban wireless fading channel, channel delay spread (T_m) may be, e.g., 2 μs, i.e., coherence bandwidth $((\Delta f)_c)$ may be on the order of 100 kHz. In this example, with subcarrier width $\Delta f = (700/N)$ kHz and $(\Delta f)_c = 100$ kHz, flat fades over each subcarrier are achieved with, e.g., $N \geq 15 (\Delta f < 2(\Delta f)_c)$. Next, referring to criteria 2), we minimize the time duration over which the bit energy is spread. As shown in the next paragraphs, bit energy is spread over duration NT_b: hence, with, e.g., $N \geq 15$ to ensure a flat fade, we select $N = 15$ to minimize the energy spread (in time) of each bit.

The CI/FSK signal for the zeroth bit, $a_0 \in \{-1, +1\}$, corresponds to (in the time domain)

$$s_0(t) = A \sum_{i=1}^{N} \cos\left(2\pi f_c t + a_0 \left(2\pi \left(i - \frac{1}{2}\right) \Delta f\right) t\right), \quad 0 \leq t < NT_b \tag{1}$$

where A is a constant that determines the symbol energy. Note that the signal energy is spread over the time duration NT_b, instead of the usual T_b. Here, $s_0(t)$, the sum of a finite number of sinusoids with spacing Δf, is a periodic signal with period $1/\Delta f (1/\Delta f = NT_b)$: the limitation $0 \leq t < NT_b$ holds $s_0(t)$ to a single period.

Using simple summation rules, the CI/FSK signal in (1) can be expressed in time according to

$$s_0(t) = A \frac{\sin\left(\frac{N}{2}\Delta f t\right)}{\sin\left(\frac{1}{2}\Delta f t\right)} \cos\left(2\pi \left(f_c + a_0 \frac{N}{2} \Delta f\right) t\right), \quad 0 \leq t < NT_b. \tag{2}$$

As is evident from (2), a single CI/FSK-modulated signal does not have a constant envelope. This signal $s_0(t)$ is shown (over time duration NT_b) in the solid line of Fig. 2. The CI/FSK signal can be rewritten in a more conventional manner via

$$s_0(t) = A \cdot E(t) \cos\left(2\pi (f_c + a_0 f_d) t\right), \quad 0 \leq t < NT_b \tag{3}$$

where $E(t) = (\sin((N/2)\Delta f t)/\sin((1/2)\Delta f t))$ represents the CI envelope pattern, and $f_d = (N/2)\Delta f = (N/2)\cdot(1/NT_b) = (1/2T_b)$.

B. Bit-Stream Transmission

Next, we consider the transmission of a bit stream. Following transmission of the zeroth bit, the first bit is sent as [referring to (3)]

$$s_1(t) = A \cdot E(t - T_b)\cos(2\pi(f_c + a_1 f_d)t), \quad 0 \le t < NT_b. \tag{4}$$

This is illustrated in Fig. 2 over duration 0 to NT_b via the dotted line. It is easily shown that

$$\int_0^{NT_b} E(t - kT_b)E(t - nT_b)dt = 0, \quad (n \ne k). \tag{5}$$

Hence, a bit stream modulated using CI/FSK maintains the required condition of zero ISI [by satisfying the generalized Nyquist criterion (GNC)] at the transmitter side, i.e., $s_0(t)$ and $s_1(t)$ are orthogonal at the transmitter side. It is important to note that phase continuity is not guaranteed in CI/FSK. However, the spectral leakage is minimal, and is not viewed as a problem in CI/FSK system design. The total transmitted signal for a block of N bits then corresponds to

$$\begin{aligned} s(t) &= \sum_{k=0}^{N-1} s_k(t) \\ s(t) &= \sum_{k=0}^{N-1} A \cdot E(t - kT_b)\cos(2\pi(f_c + a_k f_d)t), \\ &\quad 0 \le t < NT_b. \end{aligned} \tag{6}$$

Expressing this in terms of the MC signal of (1), $s(t)$ can alternatively be expressed via

$$\begin{aligned} s(t) = \sum_{k=0}^{N-1} A \sum_{i=1}^{N} \cos\Bigg(2\pi f_c t + a_k \left(2\pi\left(i - \frac{1}{2}\right)\Delta f\right) \\ \times \left(t - kT_b\right)\Bigg), \quad 0 \le t < NT_b. \end{aligned} \tag{7}$$

Hence, while bit energy is spread over duration NT_b via modulation to CI/FSK, N orthogonal CI/FSK symbols are located in NT_b, leading to a throughput consistent with traditional FSK systems.

C. Pseudo-Orthogonality in CI/FSK

From (5), it is evident that the CI/FSK system supports N orthogonal modulated symbols positioned at $\{kT_b, k = 0, 1, \ldots, N-1\}$ in duration $t \in [0, NT_b]$. It is possible to support additional CI/FSK symbols in $t \in [0, NT_b]$ by positioning the modulated CI/FSK symbols pseudo-orthogonally, i.e., positioning CI/FSK symbols at times τ_k and τ_j such that we select $\tau_k - \tau_j < T_b$, and we ensure $\int_0^{NT_b} E(t - \tau_k)E(t - \tau_j)dt \le \epsilon$, where ϵ is some small predetermined value.

We allow the first N CI/FSK symbols to be placed orthogonally, i.e., their envelopes $E(\cdot)$ are transmitted with delays $\{\tau_k = kT_b, k = 0, 1, \ldots, N-1\}$. Now, if we introduce an additional delay ζ to all envelopes, i.e., replace *each* $\tau_k = kT_b$ by $\tau_k = kT_b - \zeta$ in $E(t - \tau_k)$, the set of N CI/FSK symbols remain orthogonal to one another. That is, the crosscorrelation between the signal envelopes remains zero, as long as the difference is $\tau_m - \tau_n = (mT_b - \zeta) - (nT_b - \zeta) = (m - n)T_b$. Of course, there is correlation between an orthogonal set of N envelopes with $\zeta = 0$ and the orthogonal set of N envelopes constructed with arbitrary ζ.

We seek to support $2N$ CI/FSK symbols in duration $t \in [0, NT_b]$, by simultaneously supporting one set of N CI/FSK symbols using $E(t - kT_b - \zeta)$ with $\zeta = 0$, and another set of N CI/FSK symbols using envelopes $E(t - kT_b - \zeta)$ with $\zeta \ne 0$. That is, we intend to transmit N CI/FSK symbols in $[0, NT_b]$ using envelopes $E(t), E(t - T_b), \ldots, E(t - (N-1)T_b)$, and the second set of N symbols via envelopes $E(t - \zeta), E(t - T_b - \zeta), \ldots, E(t - (N-1)T_b - \zeta)$. To do this in an optimal fashion, we determine the value of ζ that minimizes the root mean square (rms) crosscorrelation between sets. Mathematical analysis yields an intuitively pleasing result, namely, that when positioning the $2N$ envelopes in $[0, NT_b]$, each envelope should be separated from the neighboring envelope by duration $(T_b/2)$ [i.e., $\zeta = (T_b/2)$]. This is most easily understood in terms of the transmitter output

$$\begin{aligned} s(t) = \sum_{k=0}^{2N-1} A \cdot E(t - kT_b/2)\cos(2\pi(f_c + a_k f_d)t), \\ 0 \le t < NT_b. \end{aligned} \tag{8}$$

Notice that $2N$ CI/FSK symbols are positioned in the same duration $[0, NT_b]$ and the same bandwidth by separating the CI envelopes by duration $T_b/2$, rather than the usual T_b. The success of CI/FSK "channel overloading" or "oversaturation" via pseudo-orthogonal positioning of CI envelopes will depend on how well the intentional introduction of ISI at the transmitter is combated by the receiver. The novel coherent receiver introduced in Section III offers a very good BER performance, even after doubling throughput, as shown in Section IV.

D. Bandwidth Occupancy

BFSK: FSK can be understood as FM with a carefully selected modulating waveform. The bandwidth of the modulating waveform determines the total bandwidth of transmission. For traditional BFSK, the modulating waveform is a rectangular pulse. Assuming no overlap in the BFSK spectrums for binary digits zero and one, the bandwidth required to support data rate R_b is thus [16]

$$\mathrm{BW}_{\mathrm{BFSK}} = 2f_d + 2R_b = \frac{4}{T_b}. \tag{9}$$

CI/FSK: In CI/FSK, we space N subcarriers by $\Delta f = (1/NT_b)$ to represent each binary input, allowing an overlap among subcarriers while still maintaining subcarrier orthogonality (as in OFDM [14], [15]). The ability to overlap subcarriers allows CI/FSK to achieve greater bandwidth

efficiency. Specifically, with nonoverlapping spectrum for binary digits zero and one, a data rate of R_b is supported with bandwidth

$$\mathrm{BW}_{\mathrm{CI/FSK}} = 2N\Delta f = \frac{2}{T_b}. \tag{10}$$

That is, CI/FSK demonstrates the spectral efficiency of FM with a sinc-modulating waveform [16], and hence, supports higher data rates in a given bandwidth relative to BFSK.

Specifically for a given bandwidth and considering only the spectral efficiency of CI/FSK: 1) CI/FSK supports twice the data rate of traditional BFSK; and 2) CI/FSK supports a 35% increase in data rate relative to GFSK, as proposed in Bluetooth (since $\mathrm{BW}_{\mathrm{GFSK}} = 2(\beta+1)1.04R_b = 2.7R_b = (2.7/T_b)$, assuming $\beta = 0.3$ as defined in the Bluetooth standard [17]). When the doubling in throughput via pesudo-orthogonal placement of CI/FSK symbols is also taken into consideration, a bandwidth efficiency (b/s/Hz) gain of 300% and 170% is achieved relative to BFSK and Bluetooth's GFSK, respectively.

E. Envelope in CI/FSK

Considering a block of N CI/FSK signals over $[0, NT_b]$, the transmitted signal *always* consists of a sum of N time-delayed CI envelopes (6), irrespective of data sequence. (The independence of envelope and data sequence in CI/FSK represents the key difference relative to OFDM transmission.) It is easily shown that the sum of all N envelopes results in a composite envelope corresponding to a single sine wave with frequency $N\Delta f$. Therefore, the crest factor [13] of the total CI/FSK transmitted signal over $[0, NT_b]$ is $\sqrt{2}$, equal to that in a traditional BFSK signal.

III. CI/FSK Reception

In traditional BFSK, coherent reception involves the use of two matched filters, matched to the BFSK signals corresponding to a binary one and binary zero. Also, in coherent BFSK detection, filters make use of the phase information of the received signal, and the decision variable is obtained by direct comparison of the matched-filter output values.

The coherent CI/FSK receiver operates in an entirely different manner. Fig. 3 illustrates the novel coherent receiver for CI/FSK. On the bottom branch of this receiver, the received signal is projected onto all the subcarriers constituting a binary zero. This is followed by a subcarrier combining. The combining weights are chosen to exploit frequency diversity, minimize ISI, and/or minimize noise. A similar set of operations take place on the top branch, where the subcarriers constituting a binary one are separated and combined. The output of the combiner from the bottom branch is then compared with the output of the combiner from the top branch, and a decision is made based on the relative size of these outputs. We first consider the coherent detection of the kth bit in either a slow flat-fading channel or an additive white Gaussian noise (AWGN) channel. We assume the transmitted signal of either (6) or (8). Hence, the received signal corresponds to

$$r(t) = \alpha s(t) + n(t), \quad 0 \le t < NT_b \tag{11}$$

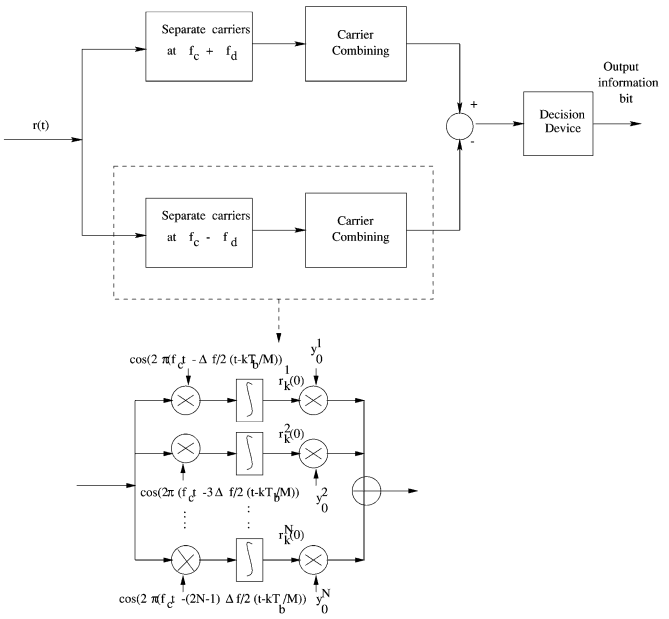

Fig. 3. Coherent receiver for detection of CI/FSK symbols.

where $s(t)$ is as represented in (6) or (8), $n(t)$ is AWGN, and α is the channel fade ($\alpha = 1$ in an AWGN channel). [Perfect phase estimation and removal has been assumed in (12)]. That is

$$r(t) = \alpha \sum_{k=0}^{K-1} AE(t - kT_b/M) \cdot \cos\left(2\pi(f_c + a_k f_d)t\right) + n(t), \quad 0 \le t < NT_b \tag{12}$$

$$r(t) = \alpha \sum_{k=0}^{K-1} A \sum_{i=1}^{N} \cos\left(2\pi f_c t + a_k\left(2\pi\left(i - \frac{1}{2}\right)\Delta f\right) \cdot (t - kT_b/M)\right) + n(t), \quad 0 \le t < NT_b \tag{13}$$

where $K = N$ and $M = 1$, if $s(t)$ corresponds to transmission of orthogonal CI/FSK symbols [(6)], and $K = 2N$ and $M = 2$, if $s(t)$ corresponds to pseudo-orthogonal transmission [(8)].

On the bottom branch of the receiver in Fig. 3 (illustrated for detection of the kth bit), a separation into subcarriers with delays matched to the kth bit is the first operation. This leads to the ith subcarrier component

$$r_k^i(0) = \alpha A \beta_k(0) + \alpha A \sum_{j=0, j\neq k}^{K-1} \beta_j(0)\rho_{j,k}^i + \eta_i(0) \tag{14}$$

where $\eta_i(0)$ is a Gaussian random variable with mean 0 and variance σ_n^2. Additionally, $\beta_k(0)$ represents the presence of binary data on the bottom branch, i.e., $\beta_k(0) = 1$ if $a_k = -1$, and $\beta_k(0) = 0$ if $a_k = 1$. The second term represents the ISI due to other information bits in $[0, NT_b]$, and $\rho_{j,k}^i = \cos\left(2\pi i \Delta f(jT_b/M - kT_b/M)\right)$ represents the crosscorrelation between the kth bit and jth bit in the ith carrier.

The subcarrier components are combined (on the bottom branch) according to

$$D_k(0) = \sum_{i=1}^{N} r_k^i(0) \cdot y_0^i. \tag{15}$$

In the upper branch, similar carrier decomposition and recombining is performed, leading to

$$D_k(1) = \sum_{i=1}^{N} r_k^i(1) \cdot y_1^i. \tag{16}$$

Here, y_0^i and y_1^i represent the combining weights in the lower branch of Fig. 3 and the upper branch of Fig. 3, respectively. $D_k(0)$ and $D_k(1)$ are then compared, and the final decision $\hat{a}_k$ corresponds to $\hat{a}_k = 1, D_k(1) > D_k(0)$, and $\hat{a}_k = -1$, otherwise.

In the case of $K = N$ orthogonal CI/FSK symbols and an AWGN or flat-fading channel, equal-gain combining (EGC), i.e., $y_1^i = y_0^i = 1$, is optimal since it maximizes the SNR, and it eliminates the ISI entirely. In the case of $K = 2N$ pseudo-orthogonal CI/FSK symbols over AWGN or flat-fading channels, a minimum mean-squared error (MMSE) combining, which jointly minimizes the noise and ISI terms, is optimal. Here

$$\begin{aligned} y_0^i &= \frac{\alpha}{\left(\alpha^2\sigma_\beta^2 \sum_{j=0}^{2N-1}\left(\rho_{j,k}^i\right)^2 + \sigma_n^2\right)} \\ y_1^i &= \frac{\alpha}{\left(\alpha^2\sigma_\beta^2 \sum_{j=0}^{2N-1}\left(\rho_{j,k}^i\right)^2 + \sigma_n^2\right)} \end{aligned} \tag{17}$$

where $\sigma_\beta^2 = A/4$ is the variance of the Bernoulli distributed variable $\beta_n(0)$ or $\beta_n(1)$.

The novel coherent receiver can also be employed in multipath fading channels with encouraging performance results. Specifically, in CI/FSK, the frequency selectivity over the entire bandwidth is resolved by the narrowband subcarriers. This will enable the coherent CI/FSK receiver to exploit the available frequency diversity (in much the same way MC-CDMA receivers benefit from frequency-diversity gains [18]–[21]).

Assume the transmitted signal of (6) or (8) is sent over a frequency-selective (multipath) slow-fading channel. Here, frequency selectivity corresponds to selectivity over the entire transmit bandwidth, but not over each individual subcarrier making up the CI/FSK symbol. That is, the ith subcarrier experiences a unique flat fade, characterized by Rayleigh distributed gain α_i and phase distortion ϕ_i. (This is typical of MC signals; see, e.g., the MC-CDMA and OFDM literature [14], [21]). In this case, the received signal corresponds to (assuming ideal phase tracking and removal)

$$\begin{aligned} r(t) = \sum_{k=0}^{K-1}\sum_{i=1}^{N} \alpha_i A \cos\Bigg(&2\pi f_c t \\ &+ a_k\left(2\pi\left(i-\frac{1}{2}\right)\Delta f\right)(t - kT_b/M)\Bigg) + n(t). \end{aligned} \tag{18}$$

The fades on the N subcarriers corresponding to a binary one are correlated with one another, and also with the fades on the N subcarriers corresponding to a binary zero. The degree of correlation is based on coherence bandwidth, and is characterized as seen in [22] and [23]. (Correlated fades may be generated based on the algorithm provided in [24]).

We employ the coherent receiver of Fig. 3 to detect the kth bit from the received signal of (19). Considering the bottom branch in the receiver of Fig. 3, the received signal is first decomposed into its subcarriers, where each subcarrier displays a delay matched to the kth bit. The ith subcarrier component is easily shown to correspond to

$$r_k^i(0) = \alpha_i(0)A\beta_k(0) + \alpha_i(0)A\sum_{j=0, j\neq k}^{N-1}\beta_j(0)\rho_{j,k}^i + \eta_i(0) \tag{19}$$

where $\alpha_i(0)$ represents the fade on the subcarrier with frequency $f_c - (i-1/2)\Delta f$ (i.e., $\alpha_i(0)$ matches the α_i of (19) if $a_k = -1$, and $\alpha_i(0)$ represents a fade correlated with, but different from, the α_i of (19) if $a_k = +1$). All other variables in (20) are as defined in (15). The $r_k^i(0)$ terms are combined across carriers to create the decision variable $D_k(0)$, as shown in (16). A similar set of operations performed along the top branch lead to decision variable $D_k(1)$. Unlike the AWGN scenario, EGC is no longer a suitable combining strategy, because the introduction of carrier-dependent fades α_i destroys the orthogonality between CI/FSK symbols. Hence, we attempt to jointly exploit frequency diversity, and minimize the ISI and noise terms in (20) via a MMSE combiner. Wiener filter theory analysis yields the following weights:

$$\begin{aligned} y_0^i &= \frac{\alpha_i^0}{\left(\left(\alpha_i^0\right)^2\sigma_\beta^2 \sum_{j=0}^{K-1}\left(\rho_{j,k}^i\right)^2 + \sigma_n^2\right)} \\ y_1^i &= \frac{\alpha_i^1}{\left(\left(\alpha_i^1\right)^2\sigma_\beta^2 \sum_{j=0}^{K-1}\left(\rho_{j,k}^i\right)^2 + \sigma_n^2\right)}. \end{aligned} \tag{20}$$

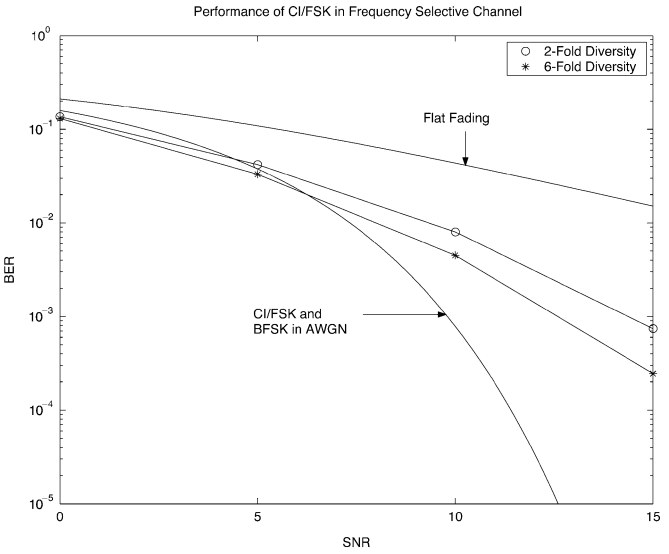

Fig. 4. CI/FSK performance in frequency-selective channel with different degrees of diversity.

IV. Performance Results

Performance results are characterized using BER versus SNR curves. Here, we compare traditional BFSK performance curves to those of an orthogonal CI/FSK (O-CI/FSK) system, where $N = 15$ O-CI/FSK symbols are transmitted in every duration $[0, 15T_b]$, and a pseudo-orthogonal CI/FSK (PO-CI/FSK)

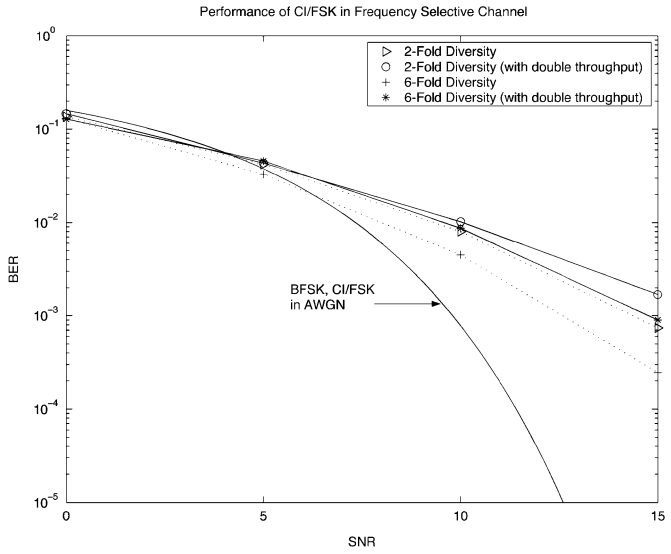

Fig. 5. CI/FSK performance in frequency-selective channels with double throughput.

system, where $N = 30$ symbols are sent in every $[0, 15T_b]$ duration (by pseudo-orthogonal positioning of CI/FSK symbols).

Figs. 4 and 5 represent the BER curves for O-CI/FSK and PO-CI/FSK in frequency-selective channels, assuming coherent reception of Fig. 3. Specifically, Fig. 4 plots O-CI/FSK performance, demonstrating the improvement in performance with increasing diversity (the degree of diversity, L, is defined as the ratio between the transmission bandwidth per bit $(N\Delta f)$ and coherence bandwidth of the channel $(\Delta f)_c$). (In terms of delay spread, sixfold diversity corresponds to a channel with rms delay spread of $1.2T_b$; and twofold diversity corresponds to a channel with rms delay spread of approximately $0.5T_b$.) As rms delay spread increases, the performance of CI/FSK improves (moving toward the AWGN performance limit). Furthermore, it is important to remember that these performance gains are achieved alongside a doubling in throughput relative to BFSK (consequence of spectral efficiency in O-CI/FSK). In Fig. 5, PO-CI/FSK supports $2N = 30$ CI/FSK symbols in each duration $15T_b$. We observe that, in this case, performances are close to those with a twofold diversity gain in O-CI/FSK.

Overall, we observe that O-CI/FSK doubles throughput relative to BFSK without performance degradation due to improved spectral efficiency; O-CI/FSK exploits diversity gains and drives performance away from the poor flat-fading results (and toward the excellent AWGN performances); and PO-CI/FSK operating over frequency-selective fading channels achieves performance curves consistent with twofold diversity benefits, while offering a fourfold gain in throughput.

V. Conclusion

In this letter, we presented an innovation in FSK architecture in the form of a MC implementation. Specifically, the new CI/FSK scheme involves transmission of multiple orthogonal subcarriers around two carrier frequencies to represent binary information. This scheme is spectrally efficient relative to traditional FSK, and further supports increased throughputs through pseudo-orthogonal symbol positioning. The CI/FSK architecture also maintains excellent crest factors (peak-to-average power ratios). Finally, the novel coherent receiver designed for CI/FSK makes it suitable for use in frequency-selective channels, with the system benefiting from the available frequency diversity and providing excellent BER performance at high data rates.

References

[1] E. A. Lee and D. G. Messerschmitt, *Digital Communications*. Norwell, MA: Kluwer, 1990.
[2] *Specification of the Bluetooth System*, Bluetooth SIG group, ver. 1.0 draft foundation, July 1999.
[3] J. C. Haartsen and S. Mattisson, "Bluetooth—A new low-power radio interface providing short-range connectivity," *Proc. IEEE*, vol. 88, pp. 1651–1661, Oct. 2000.
[4] C. Bisdikian, "An overview of the Bluetooth wireless technology," *IEEE Commun. Mag.*, vol. 39, pp. 86–94, Dec. 2001.
[5] J. Proakis, *Digital Communications*, 3rd ed. New York: McGraw-Hill, 1995.
[6] K. S. Juo, U. S. Goni, and A. M. D. Turkmani, "Comparative evaluation of the performance of anti-multipath modulation techniques for digital mobile radio systems," in *Proc. IEEE Vehicular Technology Conf.*, Stockholm, Sweden, June 1994, pp. 1557–1561.
[7] P. S. K. Leung, "Asymmetric-raised-cosine frequency-shift keying (ARC-FSK)—A new modulation with superior anti-multipath characteristics for mobile and personal communications systems," in *Proc. 4th IEEE Int. Conf. Universal Personal Communications*, 1995, pp. 117–122.
[8] F. Danila and H. Leib, "FSK and DPSK over unresolved multipath Rayleigh fading channels," in *Proc. 6th IEEE Int. Symp. Personal, Indoor, Mobile Radio Communications*, vol. 2, 1995, pp. 477–481.
[9] R. Petrovic and A. F. Molisch, "Reduction of multipath effects for FSK with frequency discriminator detection," in *Proc. 6th IEEE Int. Symp. Personal, Indoor, Mobile Radio Communications*, vol. 3, 1995, pp. 943–481.
[10] M. K. Varanasi, "Noncoherent equalization for multipulse modulation," in *Proc. IEEE Int. Conf. Personal Wireless Communications*, 1997, pp. 218–222.
[11] V. A. Aalo and J. Zhang, "Performance of maximal-ratio combining diversity in a Nakagami fading channel with cochannel interference," in *Proc. IEEE Wireless Communications, Networking Conf.*, vol. 1, 1999, pp. 1–5.
[12] Y. Xin, S. Zhang, M. K. Simon, and M.-S. Alouini, "Average BER performance of noncoherent orthogonal MFSK over Nakagami fading channels," in *Proc. IEEE Wireless Communications, Networking Conf.*, vol. 3, 2000, pp. 1065–1069.
[13] E. V. Ouderaa, J. Schoukens, and J. Renneboog, "Peak factor minimization of input and output signals of linear systems," *IEEE Trans. Instrum. Meas.*, vol. IM-37, pp. 207–212, June 1988.
[14] K. Sathanathan and C. Tellambura, "Probability of error calculation of OFDM systems with frequency offset," *IEEE Trans. Commun.*, vol. 49, pp. 1884–1888, Nov. 2001.
[15] B. Le Floch, M. Alard, and C. Berrou, "Coded orthogonal frequency-division multiplex," *Proc. IEEE*, vol. 83, pp. 982–996, June 1995.
[16] T. S. Rappaport, *Wireless Communications—Principles and Practice*, 1st ed. Englewood Cliffs, NJ: Prentice-Hall, 1996.
[17] B. Natarajan, C. R. Nassar, and S. Shattil, "Enhanced Bluetooth and IEEE 802.11(FH) via multicarrier implementation of the physical layer," in *Proc. IEEE Emerging Technologies Symp.*, Richardson, TX, Sept. 10–11, 2001, pp. 129–133.
[18] S. Hara and R. Prasad, "Overview of multicarrier CDMA," *IEEE Commun. Mag.*, vol. 35, pp. 126–133, Dec. 1997.
[19] S. Hara and R. Prasad, "DS-CDMA, MC-CDMA, and MT-CDMA for mobile multimedia communications," in *Proc. Vehicular Technology Conf.*, Atlanta, GA, Apr. 1996, pp. 1106–1110.
[20] K. Fazel, S. Kaiser, and M. Schnell, "A flexible and high-performance mobile communications system based on orthogonal multicarrier SSMA," *Wireless Pers. Commun.*, vol. 2, pp. 121–144, 1995.
[21] N. Yee, J. P. Linnartz, and G. Fettweis, "Multicarrier CDMA in indoor wireless radio," in *Proc. PIMRC*, Yokohama, Japan, Dec. 1993, pp. 109–113.
[22] W. C. Jakes, *Microwave Mobile Communications*. New York: IEEE Press, 1974.
[23] W. Xu and L. B. Milstein, "Performance of multicarrier DS-CDMA systems in the presence of correlated fading," in *Proc. IEEE 47th Vehicular Technology Conf.*, Phoenix, AZ, May 4–7, 1997, pp. 2050–2054.
[24] B. Natarajan, C. R. Nassar, and V. Chandrasekhar, "Generation of correlated Rayleigh fading envelopes for spread-spectrum applications," *IEEE Commun. Lett.*, vol. 4, pp. 9–11, Jan. 2000.